



CHORUS

This is the accepted manuscript made available via CHORUS. The article has been published as:

Searching for optimal THz generation through calculations of the asymmetry of photoelectron momentum distributions by an improved strong-field-approximation method

Zhaoyan Zhou, Dongwen Zhang, Jinlei Liu, Zengxiu Zhao, and C. D. Lin

Phys. Rev. A **107**, 013106 — Published 13 January 2023

DOI: [10.1103/PhysRevA.107.013106](https://doi.org/10.1103/PhysRevA.107.013106)

Searching for optimal THz generation through calculations of the asymmetry of photoelectron momentum distributions by improved strong-field approximation method

Zhaoyan Zhou,^{1,*} Dongwen Zhang,¹ Jinlei Liu,¹ Zengxiu Zhao,¹ and C. D. Lin²

¹*Department of Physics, College of Science, National University of Defense Technology, 410073 Changsha, P. R. China*

²*Department of Physics, Cardwell Hall, Kansas State University, Manhattan, Kansas 66506, USA*

(Dated: January 3, 2023)

From solving the time-dependent Schrödinger equation (TDSE), it has been shown that in a two-color laser pulse the relative phase that optimizes THz radiation also optimizes the asymmetry of the angular distribution of photoelectrons. Here, we show that a second-order strong field approximation (SFA2) can accurately calculate the asymmetry of photoelectrons and thus can locate the phase delay that optimizes THz generation, which is four orders of magnitude faster than from TDSE calculations. We further trace that this is possible because THz emission originates from free-free radiative transition between the rescattered electron with the target ion, similar to other electron-ion collisions in the laser field, e.g., high harmonic generation and nonsequential double ionization. Our results pave the way to locate the optimal phase delay for any typical laser pulses for maximal THz generation in the laboratory.

PACS numbers: 32.80.Rm, 42.65.Re, 52.38.-r

I. INTRODUCTION

Terahertz(THz) radiation has a wide range of applications in pharmaceutical, automotive, biological imaging and other fields due to its unique properties such as low photon energy, no absorption in non-polar materials, and its coverage over vibrational and rotational energies of many organic and inorganic macromolecules[1, 2]. Intense THz pulses with broad bandwidth can be generated in gas driven by strong asymmetric two-color laser fields [3–6]. The mechanism for THz generation has been modeled initially by the photocurrent (PC) model as due to the DC component of the ionized electrons [7]. In this classical PC model, the current is obtained by solving Newton’s equations for free electrons in the laser field. Ignoring the role of Coulomb potential and treating ionized electrons as free particles, the asymmetry of the laser field’s vector potential determines the asymmetry of photocurrent. In this simple PC model, THz yield reaches maximum when the asymmetry of the current is largest, which occurs when the phase delay between the two-color lasers is 0.5π .

To test the validity of the PC model, photocurrents of the ionized electrons have been calculated “exactly” by solving the time-dependent Schrödinger equation (TDSE), from which the intensity of THz waves is obtained[8–11]. These calculations, together with later experiments, found that the phase delay that generates the maximal THz yield is not 0.5π , but is about 0.8π . Additional TDSE calculations also showed that THz radiation depends on other laser parameters besides the phase delay, like the relative field strength, and their

relative frequencies[11–14]. These quantum calculations also established that THz yields depend not only on the asymmetric vector potential of the laser, but also on the ionic potential of the target atom. Unlike other strong field phenomena, theoretical calculations on THz generation have been carried out mostly by solving TDSE so far, such that the mechanism of THz generation remains unclear. Simpler models commonly used in strong field physics, for example, the strong field approximation (SFA)[15], have not been found to be relevant in THz generation.

To understand the mechanism of THz generation, we first review the well-understood models used in describing strong field phenomena[16]. In a strong laser field, an electron is readily ripped off from the atom by the laser field, which may directly escape from the ion and drift to the detector. These electrons are called escaping electrons or direct electrons. In this simplest model, one assumes the ion potential does not affect the escape of the free electron such that the momentum distribution of the photoelectron is governed by the vector potential of the laser[17, 18]. These electrons have low energies. According to the classical model, the cutoff energy of direct electron is given by $2U_p$ [19, 20], where U_p is the instantaneous Ponderomotive energy. However, tunnel-ionized electrons can be driven back to recollide with the ion to initiate various electron-ion rescattering processes, such as high-order harmonic generation (HHG), high-energy photoelectrons that lead to laser-induced electron diffraction (LIED)[21, 22] and nonsequential double ionization (NSDI)[16]. These are well-known electron-ion collision processes for radiative recombination, elastic electron-ion backscattering and electron-impact ionization, respectively, except that the collisions occur in the laser field. So what is the physical process that generates THz radiation? Clearly, a free electron cannot

*Email:cnzhzhy@nudt.edu.cn

spontaneously break into a photon and another electron as it would violate conservation of energy and momentum together. A free electron can collide with an ion to emit radiation accompanied by a change of electron momentum since the ion would recoil to conserve energy and momentum. This process is alternatively understood as bremsstrahlung in which radiation is emitted when an electron is slowed down by an external field. In electron collision language, it is called free-free radiation process. Thus, THz radiation, like HHG, LIED, NSDI, all belong to electron-ion collision processes in the laser field. This point actually has been mentioned in the original photocurrent model[7], but it did not clearly state how the current was to be calculated.

In strong field physics, the rescattering is understood with the so-called three-step model: (1) tunnel ionization, (2) free propagation of electrons in the laser field, (3) electron collisions with the ions. This model has been re-casted in the so-called quantitative rescattering theory (QRS)[23–26]. In QRS, after tunnel ionization, a fraction of the electrons will be driven back to recollide with the ion. These currents are similar to incident laboratory currents in electron collisions. For THz generation, the “incident” currents from “left” and “right” sides of the polarization axis should be different, and THz yields are proportional to the asymmetry of the returning current from the two sides.

The separation of electrons after tunnel ionization into direct electrons and rescattered electrons is most conveniently done by taking the electron-ion interaction potential as perturbation in a strong laser field. In the first-order strong field approximation (SFA1)[27–30] the ionized electron does not expose to the force from the ion. To account for electron-ion collisions in the laser field, a second-order strong field approximation (SFA2) is needed. (see Section II below and [16]). According to the QRS model, the photocurrent can be calculated from the high-energy photoelectron spectra using the SFA2. For THz radiation, SFA2 can also be applied to low-energy electrons which result from forwardly scattered photoelectrons[31, 32]. Since THz strength, according to the photocurrent model, comes from rescattering electrons, which in turn can be calculated from SFA2. Thus, the search of phase delay which can optimize THz emission can be obtained directly from the phase delay of the two-color pulse that would give the optimal asymmetry in photoelectrons. Since SFA2 calculations are at least four orders of magnitude faster, it provides a quick way to locate the phase delay that would generate optimal THz for any lasers.

We remark that our conclusion is consistent with the results reported in [13, 14]. These authors solved the classical Newton equation to obtain the current of an atom in a strong two-color field in the presence of a Coulomb potential. They analyzed the electron trajectory for each calculation to identify whether the electron just escapes to the detector, or has undergone a collision. They are called escaping electrons, and (soft) rescattered collision

electrons, respectively. As shown in Fig. 4(b) of [13] and Fig. 9(c) of [14], they found that THz yields from escaping electrons are nearly zero for all phase delays, while the THz yields obtained from the rescattered electrons are in fair agreement with those calculated from solving the TDSE. Their analysis is consistent with our conclusion on SFA1 and SFA2 contributions for THz emission discussed above.

In the rest of this article, we first outline SFA1 and SFA2. We then use SFA2 to calculate the asymmetry of photoelectron spectrum under different laser field combinations. The results are compared to 3D-TDSE calculations for a few cases. After verifying the validity of the SFA2 method, we present several examples of the dependence of THz emission efficiency on the laser parameters which would help identify optimal parameters for stronger THz emissions for two-color and three-color fields. We conclude the article by a summary on the robustness of this method.

II. THEORETICAL METHODS

In order to simulate the dynamics of electrons in strong laser fields and the associated nonlinear physical phenomena, methods of solving TDSE and SFA are used. The former is purely numerical and mainly used to verify the reliability of the results of the latter, and its numerical method has been presented previously[33]. Using the SFA method, the probability of an ATI electron (or photoelectron) with momentum \mathbf{p} can also be approximated by two terms[17, 19, 23, 33],

$$f(\mathbf{p}) = f^{(1)} + f^{(2)} \quad (1)$$

where the first term

$$f^{(1)} = -i \int_{-\infty}^{\infty} dt \langle \chi_{\mathbf{p}}(t) | H_i(t) | \Psi_0(t) \rangle \quad (2)$$

corresponds to the standard SFA method and is called as SFA1 in this paper. Here $H_i(t)$ is the laser-atom interaction. It describes the transition amplitude of directly ionized electron with momentum \mathbf{p} . The maximum energy the ATI electron can reach is $2U_p$. Without considering the Coulomb potential, the asymmetry of ATI spectrum calculated by SFA1 can only be affected by the asymmetry of the vector potential of the laser field[17, 18].

The second term is SFA2,

$$f^{(2)} = - \int_{-\infty}^{\infty} dt \int_{-\infty}^t dt' \int d\mathbf{k} \langle \chi_{\mathbf{p}}(t) | V | \chi_{\mathbf{k}}(t) \rangle \times \langle \chi_{\mathbf{k}}(t') | H_i(t') | \Psi_0(t') \rangle. \quad (3)$$

This expression can be understood by reading it from the right side. The electron is first ionized at time t' in the laser field. It then propagates in the laser field from t' to t . Then it interacts with the atomic potential V into a state with momentum \mathbf{p} . After the interaction with the

atomic potential, the electron can reach maximal energy of $10U_p$ according to the classical rescattering model[19, 20].

It should be pointed out that in this approximation, the interaction of the electron with the atomic potential is treated only to the first order. The electron may return and interact with the atomic potential many times under the periodic laser field which is not included in the SFA2 theory. Since the electron wave packet broadens with time, such multiple scattering at later times is expected to have smaller contributions.

Within the single-electron model, the atomic potential $V(\mathbf{r})$ is taken from[34, 35]

$$V(\mathbf{r}) = -\frac{Z + a_1e^{-a_2r} + a_3re^{-a_4r} + a_5e^{-a_6r}}{r}, \quad (4)$$

where Z is the charge of the nucleus. For atomic hydrogen, $V(\mathbf{r})$ is a pure Coulomb potential. For a many-electron atom, the other parameters a_i are obtained by fitting the numerical potential calculated from the self-interaction free density function theory for different noble gases.

The momentum distribution of the emission of an electron of energy $E = p^2/2$ in the direction of $\hat{\mathbf{p}}$ is given by

$$\frac{\partial^2 P}{\partial E \partial \hat{\mathbf{p}}} = |f|^2. \quad (5)$$

The yields of directly ionized electrons or the scattered electrons can be distinguished by taking the modulus squared values of $f^{(1)}$ or $f^{(2)}$, respectively.

For a linearly polarized laser field, the system has cylindrical symmetry. The two-dimensional momentum distribution is defined by

$$\frac{\partial^2 P}{\partial E \partial \theta} = \frac{\partial^2 P}{\partial E \partial \hat{\mathbf{p}}} 2\pi p \sin \theta, \quad (6)$$

where θ is the angle between the polarization axis of the laser field and the direction of the ejected photoelectron. We can set $\theta = 0$ and π to get the signal of the photoelectron (P_+) along the laser polarization direction and then calculate the asymmetry parameter by

$$A = (P_+ - P_-)/(P_+ + P_-). \quad (7)$$

In the above equation, the asymmetry can be defined with respect to a specific photoelectron energy, or with respect to a range of energies.

III. RESULTS AND DISCUSSION

A. Asymmetry of photoelectron spectra calculated using the SFA2 theory

Many previous simulations on ATI spectrum by SFA2 method have focused on the energy distribution of

backscattered electrons whose energy is mainly distributed between $4U_p$ to $10U_p$ [17, 23, 26]. The high energy derives mainly from the additional drift momentum gained by the electron from the time of back scattering till the end of the laser pulse. The influence of atomic potential on rescattering is manifested by the elastic scattering cross-section [23, 26, 36]. The low energy electron can be generated by direct tunneling (SFA1) or by the soft collision process (SFA2). These soft-recollision electrons result from forward scattering of the electrons by the ion core, they have lower energy because its momentum is reduced by the drift momentum of the laser field. Such collisions occur at large impact parameters and thus it is classified as soft-recollision. They play an important role for understanding low-energy structure(LES)[31] and such structure has been successfully interpreted using the SFA2[32, 37].

The direct electrons, as discussed in the Introduction, do not contribute to the THz emission. Thus, in employing the photocurrent model, it is not the asymmetry of the total current that is responsible for the emission of THz. In the original PC mode[7], the authors indeed stated that the current responsible for THz is similar to the current for processes of HHG and high-energy rescattering electrons that are responsible for LIED. Both HHG and high-energy photoelectron angular distributions have been extensively studied using the QRS. Thus, these currents are also responsible for THz emission and can be calculated using the QRS theory[16].

To verify this idea, we first calculate the ATI spectrum using SFA2 for a hydrogen atom in a two-color laser field. The field is linearly polarized along the z axis and is given by

$$E_z(t) = E_L f(t) [\cos(\omega t) + 0.1 \cos(2\omega t + \varphi)], \quad (8)$$

where E_L is the amplitude and ω is the frequency of the incident 800 nm fundamental laser, $f(t)$ is its envelope which is chosen to have sine-square form with the duration of 20 optical cycles (o.c.). We take the relative phase delay φ to be 0.8π , which has been shown to give optimal THz radiation when the intensity of the fundamental is $I_L = 1.4 \times 10^{14} \text{W/cm}^2$ [11, 13]. Fig.1(a) shows the calculated 2D momentum distributions from SFA2. Even just with one percent of second harmonics, we notice significant asymmetry in the ATI spectra. The left-right ATI peaks along the polarization axis are shown in Fig.1(b) which exhibit pronounced asymmetry.

B. Dependence of photoelectron asymmetry on phase delay and other parameters of the two-color laser based on the SFA2 theory

The advantage of SFA2 theory over the solutions of TDSE is that the former is three to four orders of magnitude faster than the latter, thus it provides a convenient tool for probing asymmetry of photoelectron distributions over a large range of laser parameters of the

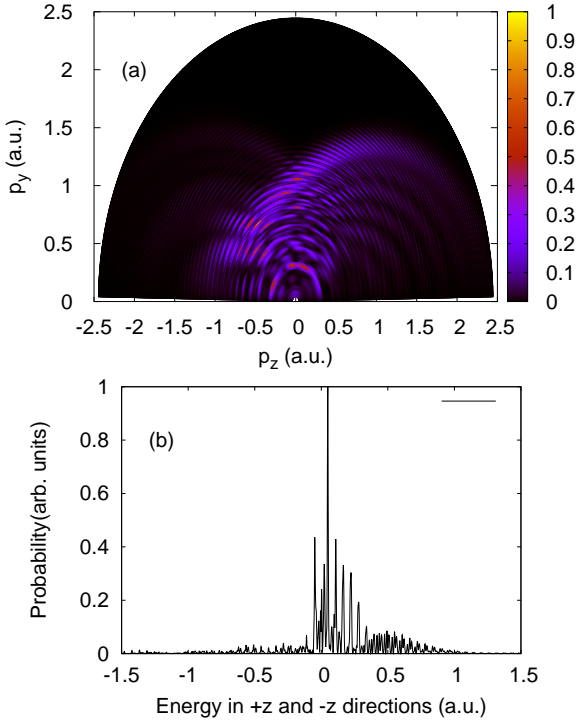


FIG. 1: (a) Photoelectron 2D momentum distributions of atomic hydrogen in parallel(p_z) and perpendicular(p_y) directions with respect to laser polarization axis. (b) The corresponding electron energy spectra on the positive and negative axes along the laser polarization direction. The two-color pulse is given by Eq. (8) where the fundamental wavelength is 800 nm and the second harmonic is 400 nm. The duration is 20 o.c. of the 800 nm, with intensity $1.4 \times 10^{14} W/cm^2$, while the the 400 nm has one percent of the fundamental. The relative phase delay between the two-color laser fields φ is chosen to be 0.8π .

two-color pulses. To begin with, we compare the normalized asymmetry of the ATI spectra integrated for photoelectrons with energies from 0 to $4U_p$ using the same laser parameters in Fig. 1, except by varying the phase delay. From Fig. 2(a), the SFA2 results mimic the THz yields obtained from solving TDSE. The agreement is quite good, thus establishing that one can use the SFA2 to calculate the ATI asymmetry in a two-color field. We comment that SFA2 implies one collision with the ion, while TDSE intrinsically implies multiple collisions with the ion so small difference is expected.

The result shown in Fig. 2(a) has important significance on THz radiation. The mechanism of THz radiation was first interpreted using the asymmetry of photocurrent calculated by classical theory. By solving the TDSE equation in quantum calculation, the asymmetry of photocurrent was found to be due to the soft collision[13, 14]. In the meanwhile, in Ref.[38, 39], it was found that the asymmetry of photocurrent is the same as the asymmetry of the photoelectron spectra when the ATI spectra were calculated by solving the TDSE as well. The results of Fig. 2(a) show that the asymmetry of the

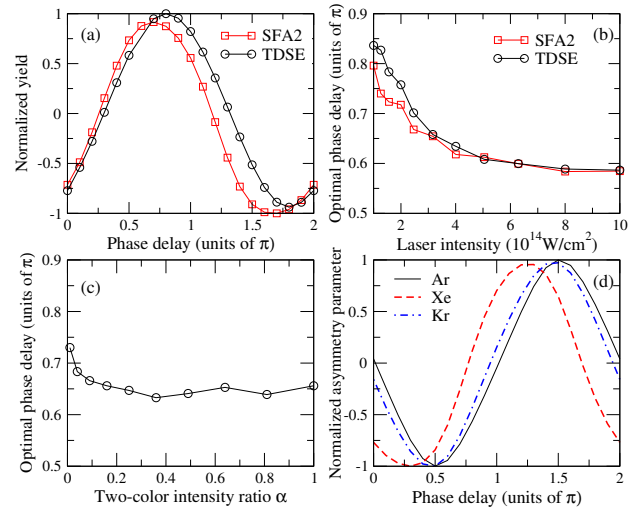


FIG. 2: (a) Comparison showing a good agreement of the normalized asymmetry parameter of the total signal of photoelectrons obtained by the SFA2 method (red-square) with the THz signals (black-circle) obtained from solving TDSE as a function of the relative phase φ for hydrogen atom. (b) Similar comparison showing a good agreement as (a) but for the optimal phase delay for the strongest THz radiation versus asymmetry calculated by SFA2 by changing laser intensity. The TDSE results in (b) are taken from Fig. 2 of Ref.[11]. (c) As in (a), but the intensity ratio was varied, showing that optimal phase does not change with the intensity ratio. (d) Phase delay dependence as in (a) but by changing the target atoms to Ar, Kr and Xe, respectively. The laser parameters are the same as those in (a).

ATI spectra can be more easily calculated directly from SFA2. This result is extremely interesting since one can study the dependence of THz emission on the properties of a two-color laser field simply just by calculating the asymmetry of ATI spectra using the simple SFA2 theory.

To support this conclusion, in Fig. 2(b), we show the optimal phase for the two-color pulse given in Eq. (8) by changing the laser intensity using SFA2 and TDSE. The TDSE results are taken from Ref. [11]. For the intensities shown, the optimal phase delay drops from about 0.8π to 0.6π , showing good agreement between TDSE and SFA2.

Using SFA2, we can then make many new predictions, for example, how the optimal phase for asymmetry in the ATI spectra depends on the relative intensity $\alpha = I_{2\omega}/I_\omega$ of the second harmonic with respect to the fundamental one. From Fig. 2(c), we found that the optimal phase appears to be fairly independent of this ratio.

The calculations shown above were all based on atomic hydrogen as the target. Next, we examine how the asymmetry of the ATI electrons depends on the target. In Fig. 2(d), we compare the asymmetry of ATI spectra of Ar, Kr and Xe, using the laser parameters as in Fig. 2(a). Comparing to Fig. 2(a), we do see non-negligible difference between H and the three rare gas atoms, but the phase-delay dependence among the three rare gas atoms does look similar except for a small shift among them. This

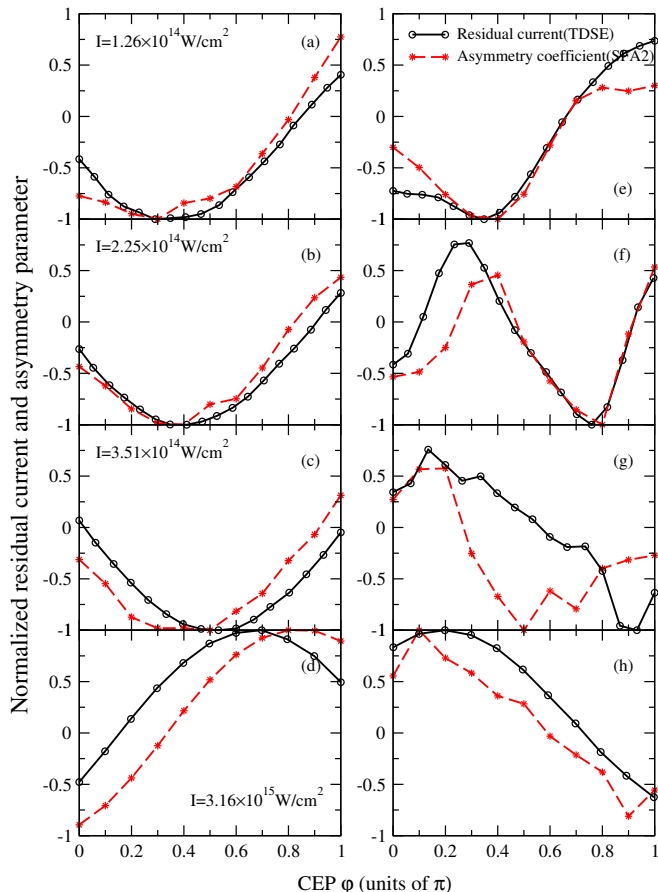


FIG. 3: The asymmetry parameter of the photoelectrons along the polarization direction (red-star dashed line) as a function of the CEP ϕ , (a)-(d) for single cycle pulses and (e)-(h) for two-cycle laser fields. The black-circle solid line represents the normalized photocurrent calculated from TDSE and is extracted from Fig. 1 of Ref. [8]. The signals are normalized for comparison.

target asymmetry dependence reflects that the electron ionization potential $V(r)$ [Eq. (4)] plays a role in SFA2. In SFA1, the potential $V(r)$ comes only in the form of the ground state wave function and thus the asymmetry is rather insensitive to the target.

C. Dependence of photoelectron asymmetry on the carrier-envelope-phase of an ultrashort one-color laser pulse

A single-color ultrashort laser pulse has asymmetric electric field that varies with the carrier-envelope phase (CEP) ϕ , thus it is also possible to generate THz and produce asymmetric ATI electron spectra. According to the classical photocurrent model, the THz radiation yield should be in proportion to $\sin \phi$ without considering the atomic potential. However, based on the 3D numerical solution of quantum TDSE, the CEP-dependence is much more complicated. TDSE calculations have

been carried out by A. A. Silaev *et al* [8] to study the CEP-dependence of THz radiation for several laser intensities and pulse durations based on the photocurrent model. Here we employ SFA2 to calculate the asymmetry of photoelectron spectra using the laser parameters in their work. In Figs. 3(a)-3(c), for single-cycle pulses (FWHM $\tau_p = 2.67 \text{ fs}$), we note that our results compare very well with their reported residual currents. The results in Fig. 3(a) also coincide with the previous researches on the asymmetries of ATI spectrum calculated by TDSE [17, 18], where the photoemission is symmetric for CEP $\phi = -\pi/3 \pm k\pi$ for ultrashort laser pulse when the laser intensity is chosen in the tunnel ionization regime but below the over-barrier ionization regime. The CEP-dependence also changes with laser intensity as shown in Figs. 3(a)-(d) because of the competition between the laser fields and atomic potentials. At the much higher intensity of $3.16 \times 10^{15} \text{ W/cm}^2$ in Fig. 3(d), while the CEP-dependence has changed a lot, the ATI asymmetry calculated from SFA2 and from TDSE remains to have similar shape.

In Figs. 3(e-h), similar asymmetries for two-cycle (FWHM $\tau_p = 5.34 \text{ fs}$) short pulses are compared between what has been reported by A. A. Silaev *et al* [8] with the ATI asymmetry calculated from SFA2 using identical laser pulses. The CEP dependence shows much faster changes as the laser intensity is increased, while larger discrepancy can be seen in the two intensities in the middle. With the two-cycle pulses, as compared to the one-cycle ones, the asymmetries of the laser pulses are much smaller, thus the calculated asymmetries of the photocurrent and of the ATI spectra are significantly smaller. [The maximal asymmetries for one-cycle pulses in Figs. 3(a-d) are about (0.6, 0.6, 0.5, 0.5) and for the two-cycle pulses in Figs. 3(e-h) are (0.25, 0.08, 0.07, 0.07)]. The small asymmetry would reduce the THz generation and lead to faster change with CEP that gives the optimal asymmetry. Such fast change of asymmetry with respect to the CEP also shows up in the fast intensity dependence in the optimal CEP as depicted in Fig. 4(b). This figure is to be compared to the smooth curve seen in Fig. 4(a) for the single-cycle pulse where the optimal phase for asymmetry stays nearly constant within the same intensity range. We comment that the asymmetry for two-cycle pulses in general is small so it is not of great interest for THz generation. In the meanwhile, experimentally, one-cycle laser pulses are more difficult to produce in the laboratories, thus generating THz radiations using a single color pulse is not expected to be of great interest.

D. Normalized asymmetry of ATI spectra in other two- and three-color fields

It has been proposed that there are other means of optimizing THz generation in a two-color field by choosing frequencies other than the commonly used $\omega_1 : \omega_2 = 1 : 2$

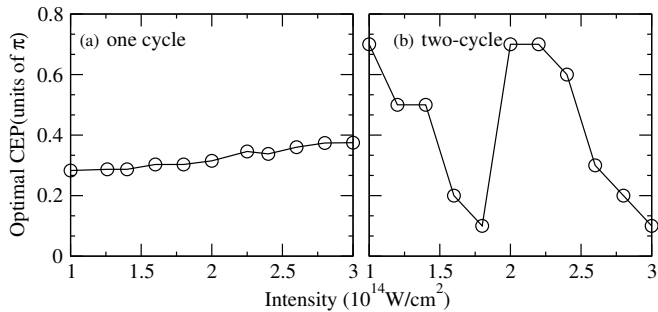


FIG. 4: The optimal carrier-envelope phase as functions of the laser intensity for (a) single cycle and (b) two-cycle laser fields.

ratio [39–43]. In our previous publication, we found that THz yield is strengthened if $n_1\omega_1 = n_2\omega_2$ and the sum of n_1 and n_2 is an odd natural number based on the multiphoton mixing theory[39]. We can also use the present method to find the optimal phases of the two pulses that would result in the highest THz radiations.

The THz radiation efficiency can also be enhanced by using well-designed multi-color laser pulses based on theoretical calculations from solving the TDSE[44]. For example, one can take a three-color laser field of the form,

$$E_z(t) = E_L f(t) [\cos(\omega t + \varphi_1) + 0.1 \cos(2\omega t + \varphi_2) + 0.1 \cos(3\omega t + \varphi_3)], \quad (9)$$

which could provide multiple pathways leading to more efficient THz generation. Clearly, there are many parameters to choose, but the relative phases are expected to be the most sensitive ones. As an example, consider the case where we first fix the phases of the fundamental and the second harmonic as $\varphi_1 = -0.5\pi$, $\varphi_2 = 0.5\pi$, and then change the phase of the third harmonic φ_3 from 0 to 2π . Here we use SFA2 to calculate the change of asymmetry parameter with the change of φ_3 . The results are compared to the asymmetry calculated by solving the TDSE, as shown in Fig. 5(a). Their general shapes are quite similar, except for a small shift. Different from the two-color case, this choice of φ_1 and φ_2 has given an initial negative drift velocity to the ionized electron. The change of φ_3 will increase or decrease this drift velocity, but its effect is not strong enough to change the direction of total photocurrent. In this case of changing φ_3 with fixed φ_1 and φ_2 , the photocurrent stays in the $-z$ direction for φ_3 varying from 0 to 2π . When the third harmonic laser field is added, it makes the electron drift in the $-z$ direction to a maximum. This will lead to the minimum DC part in the photocurrent and the THz radiation can be greatly enhanced. This is similar to what has been concluded in Ref. [44]: the optimal phase for THz radiation occurs when $\varphi_3 = 1.5\pi$ or -0.5π , when total laser pulse has sawtooth shape and can ionize electron with large drift velocity.

Using SFA2, we can also find optimal ATI asymmetry under the condition of fixing $\varphi_1 = -0.5\pi$, and varying

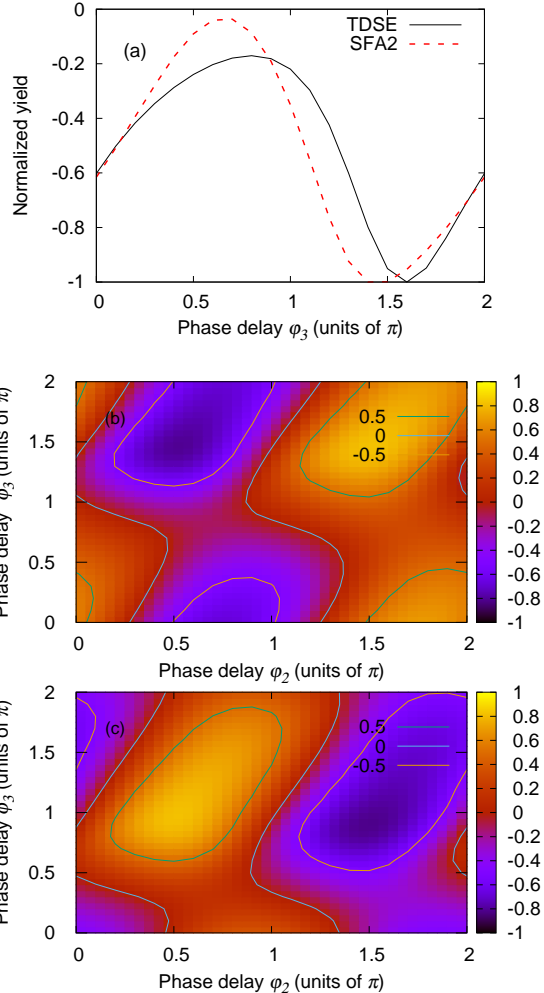


FIG. 5: (a) Comparison of the normalized asymmetry parameter of the total photoelectron (red dashed line) calculated by SFA2 with the residual photocurrent (black solid line) calculated from TDSE as a function of the relative phase φ_3 for three-color laser field of Eq. (9) where we set $\varphi_1 = -0.5\pi$ and $\varphi_2 = 0.5\pi$. The laser parameters are the same as those in Fig. 1. The intensities of the second and third harmonic laser field are both fixed to be one percent of the fundamental one. (b) The 2D asymmetry map calculated from SFA2 for the three-color pulse where φ_1 is fixed at -0.5π . The map was calculated by varying φ_2 and φ_3 simultaneously. (c) The same as (b), but φ_1 is fixed at 0.

φ_2 and φ_3 to find the optimal phase combinations for THz radiation. The result is illustrated in Fig. 5(b). For example, the drift velocity along $+z$ direction appears when φ_2 is around 1.5π , and THz radiation can also be extremely strengthened when φ_3 is chosen to be 1.5π . Instead, if φ_1 is fixed to be 0, the optimal phase combinations of φ_2 and φ_3 will change, as shown in Fig. 5(c). While the rule is similar, and THz radiation can be effectively strengthened when the choice of φ_2 and φ_3 pushes the ionizing electron to drift in the same direction. For example, when φ_2 is fixed to be 0.5π , the direction of the photocurrent remains positive whatever φ_3 is. And the photocurrent reaches the positive maximum when $\varphi_3 = \pi$.

IV. SUMMARY AND CONCLUSIONS

For years, the SFA1 theory has been used to simulate THz radiation without success, either by photocurrent theory or directly by calculating free-free transitions[15]. In previous works [38, 39], it has been found that the asymmetry of photocurrent *vs* the asymmetry of photoelectrons have common phase-angle dependence. However, these conclusions are based on solving the TDSE. In this paper, we showed that asymmetry of photoelectron distributions does not require a full solution of TDSE, but can be obtained directly from calculating SFA2. Since

calculations using SFA2 are four orders faster than solving the TDSE, we can use SFA2 calculation to map out optimal laser parameters that would generate highest THz emission. We also have used SFA2 to calculate the asymmetry of photoelectrons produced by ultrashort single-cycle pulses and obtained the best CEPs that are identical to results from solving TDSE. Due to the simplicity of obtaining asymmetry of photoelectrons from SFA2, we also demonstrated that combinations of phases of a three-color pulse can also be obtained to optimize THz generation. Finally, for the first time we put the THz generation on the same framework as the well-studied HHG, LIED and NSDI processes. They all belong to electron-ion recollisions in the laser field. Thus, the three-step model, or the QRS theory[16], should be extended to calculate THz in the future.

Acknowledgments

This work is supported by the National Natural Science Foundation of China (Grants No. 11874425, No. 12234020, No.12274461 and No. U1830206,). CDL is supported in part by Chemical Sciences, Geosciences and Biosciences Division, Office of Basic Energy Sciences, Office of Science, U. S. Department of Energy under Grant No. DE-FG02-86ER13491.

-
- [1] D. Mittleman, Sensing with Terahertz Radiation (Springer, Berlin,2003).
 - [2] J. F. Federici, B. Schulkin, F. Huang, D. Gary, R. Barat,F. Oliveira, and D. Zimdars, Semicond. Sci. Technol., 20, S266 (2005).
 - [3] X. Xie, J. Dai, and X.-C. Zhang, Phys. Rev. Lett., 96, 075005 (2006)
 - [4] J. Dai, X. Xie, and X.-C. Zhang, Phys. Rev. Lett., 97, 103903 (2006)
 - [5] D. J. Cook and R. M. Hochstrasser, Opt. Lett., 25, 1210 (2000)
 - [6] V. A. Andreeva, O. G. Kosareva, N. A. Panov, D. E. Shipilo, P. M. Solyankin, M. N. Esaulkov, P. González de Alaiza Martínez, A. P. Shkurinov, V. A. Makarov, L. Bergé, and S. L. Chin, Phys. Rev. Lett., 116, 063902(2016)
 - [7] K. Kim, J. H. Glowina, A. J. Taylor, G. Rodriguez, Opt. Express., 15, 4577 (2007)
 - [8] A. A. Silaev and N. V. Vvedenskii, Phys. Rev. Lett., 102, 115005 (2009)
 - [9] N. Karpowicz and X.-C. Zhang, Phys. Rev. Lett., 102, 093001 (2009)
 - [10] A. A. Silaev, M. Y. Ryabikin, and N. V. Vvedenskii, Phys. Rev. A, 82 , 033416 (2010)
 - [11] W. Chen, Y. Huang, C. Meng, J. Liu, Z. Zhou, D. Zhang, J. Yuan, Z. Zhao, Phys. Rev. A, 92, 033410 (2015)
 - [12] L. N. Alexandrov, M. Y. Emelin, and M. Y. Ryabikin, J. Phys. B: At. Mol. Opt. Phys. 47, 204028 (2014)
 - [13] D. Zhang, Z. Lv, C. Meng, X. Du, Z. Zhou, Z. Zhao, and J. Yuan, Phys. Rev. Lett., 109,243002(2012)
 - [14] Z. Lv, D. Zhang, C. Meng, X. Du, Z. Zhou, Y. Huang, Z. Zhao and J. Yuan, J. Phys. B: At. Mol. Opt. Phys. 46, 155602(2013)
 - [15] Z. Zhou, D. Zhang, Z. Zhao and J. Yuan, Phys. Rev. A, 79, 063413 (2009)
 - [16] C. D. Lin, A. T. Le, C. Jin, and H. Wei, Attosecond and Strong-Field Physics: Principles and Applications (Cambridge University Press, Cambridge, 2018)
 - [17] D. B. Milosevic, G. G. Paulus, and W. Becker, Opt. Express., 11, 1418 (2003)
 - [18] S. Chelkowski and A. D. Bandrauk, Phys. Rev. A 71, 053815(2005)
 - [19] W. Becker, F. Grasbon, R. Kopold, D. B. Milosevic, G. G. Paulus, and H. Walther, Adv. At. Mol. Opt. Phys. 48, 35 (2002)
 - [20] G. G. Paulus, W. Becker, W. Nicklich and H Walther, J. Phys. B: At. Mol. Opt. Phys. 27 L703(1994)
 - [21] J. Xu, Z. Chen, A6D. DiChiara, E. Sistrunk, K. Zhang, P. Agostini, T. A. Miller, L. F. DiMauro , and C. D. Lin. Nature 483, 194 (2012).
 - [22] Junliang Xu, Zhangjin Chen, Anh-Thu Le, and C. D. Lin, Phys. Rev. A 82, 033403 (2010)
 - [23] Z. Chen, A. T. Le, T. Morishita, and C.D. Lin, Phys. Rev. A 79, 033409 (2009)
 - [24] A. T. Le, R. R. Lucchese, S. Tonzani, T. Morishita, and C. D. Lin, Phys. Rev. A 80, 013401(2009)
 - [25] Z. Chen, A. T. Le, T. Morishita, and C. D. Lin, Phys. Rev. A 79, 033409(2009)

- [26] S. Micheau, Z. Chen, T. Morishita, A. T. Le, and C. D. Lin, *J. Phys. B: At. Mol. Opt. Phys.* 42, 065402 (2009)
- [27] L. V. Keldysh, *Sov. Phys. JETP* 20, 1307(1964)
- [28] F. H. M. Faizal, *J. Phys. B* 6, L89 (1973)
- [29] H. R. Reiss, *Phys. Rev. A* 22, 1786 (1980)
- [30] M. Lewenstein, Ph. Balcou, M. Yu. Ivanov, Anne LHuilier, and P. B. Corkum, *Phys. Rev. A* 49, 2117(1994).
- [31] C. I. Blaga, F. Catoire, P. Colosimo, G. G. Paulus, H. G. Muller, P. Agostini, and L. F. DiMauro, *Nature Phys* 5, 335 (2009).
- [32] W. Becker, S. P. Goreslavski, D. B. Milosevic and G. G. Paulus, *J. Phys. B: At. Mol. Opt. Phys.* 47, 204022 (2014)
- [33] Z. Chen, T. Morishita, A. T. Le, and C.D. Lin, *Phys. Rev. A* 76, 043402 (2007)
- [34] X. M. Tong, and C. D. Lin, *J. Phys. B: At. Mol. Opt. Phys.* 38, 2593(2005)
- [35] X. M. Tong, and Shih-I. Chu, *Phys. Rev. A*, 55, 3406 (1997)
- [36] Z. Zhou, X. Wang, Z. Chen, and C. D. Lin, *Phys. Rev. A* 95, 063411 (2017)
- [37] L. Guo, S. S. Han, X. Liu, Y. Cheng, Z. Z. Xu, J. Fan, J. Chen, S. G. Chen, W. Becker, C. I. Blaga, A. D. DiChiara, E. Sistrunk, P. Agostini, and L. F. DiMauro, *Phys. Rev. Lett.* 110, 013001 (2013)
- [38] Z. Zhou, X. Wang, C. D. Lin, *Phys. Rev. A*, 95, 033418 (2017)
- [39] Z. Zhou, Z. Lv, D Zhang, Z. Zhao, and C. D. Lin, *Phys. Rev. A*, 101, 043422 (2020)
- [40] W.-M. Wang, Y.-T. Li, Z.-M. Sheng, X. Lu, and J. Zhang, *Phys. Rev. E*, 87, 033108 (2013)
- [41] W.-M. Wang, Z.-M. Sheng, Y.-T. Li, Y. Zhang, and J. Zhang, *Phys. Rev. A*, 96, 023844 (2017)
- [42] V. A. Kostin, I. D. Laryushin, A. A. Silaev, and N. V. Vvedenskii, *Phys. Rev. Lett.*, 117, 035003 (2016)
- [43] L.-L. Zhang, W.-M. Wang, T. Wu, R. Zhang, S.-J. Zhang, C.-L. Zhang, Y. Zhang, Z.-M. Sheng, and X.-C. Zhang, *Phys. Rev. Lett.*, 119, 235001(2017)
- [44] P. González de Alaiza Martínez, I. Babushkin, L. Bergé, S. Skupin, E. Cabrera-Granado, C. Köhler, U. Morgner, A. Husakou, and J. Herrmann, *Phys. Rev. Lett.*, 114, 183901(2015)